Theory of translational diffusion in the nematic phase

Dagmara Sokolowska and Jozef K. Moscicki*
Smoluchowski Institute of Physics, Jagiellonian University, Reymonta 4, 30-059 Krakow, Poland
(Received 27 February 1996; revised manuscript received 1 August 1996)

A model of translational diffusion in the nematic phase is proposed. The generalized free-volume approach is used to evaluate the diffusion coefficient of a small hard-sphere tracer among monodisperse rodlike particles interacting via the Warner nematic potential. The free volume of the sample is visualized as a system of rigid tubelike shells polydisperse in length (a Cohen-Turnbull distribution) dissolved in the rodlike matrix. The equilibrium orientational distribution function of shells is found by means of the Flory lattice method. The theory is specialized to typical nematogens and is critically compared with experimental results. [S1063-651X(96)08111-1]

PACS number(s): 64.70.Md

I. INTRODUCTION

Experiments and numerical simulations have established that owing to the close packing prevailing at normal liquid densities and the short range of intermolecular repulsions compared with the range of forces of attraction, the spatial arrangements of molecules in liquids are determined first of all by the sizes and shapes of their constituent molecules, while intermolecular attractions generally have little effect on the structures of typical liquids [1–3].These findings are fundamental for a theoretical description of bulk and molecular properties of liquids. On the one hand, thermodynamic properties are commonly described by first treating the configuration for a system of ''hard'' bodies whose only interactions are via infinitely repulsive barriers upon contact with one another, while intermolecular interactions are subsequently introduced as perturbing effects only [1–7]. On the other hand, molecular-dynamics theories of liquids often follow a free-volume concept, i.e., it is assumed that each molecule is confined to a cage formed by its neighbors. The molecule rattles inside this cage until fluctuations in density enlarge the cage enough to permit a substantial displacement of the molecule. In this model, translational or rotational diffusion arises via continuous repetition of the process [8–12].

Onsager was the first to point out that, assuming sufficient elongation of the needlelike molecules, the appearance of the nematic phase might be a consequence solely of the rigidity and shape anisotropy of the constituent molecules [13]. Maier and Saupe, however, demonstrated that the presence of soft anisotropic attractive forces between molecules may also lead to the formation of the nematic phase, even for a fluid of geometrically spherical molecules [14]. In turn, Flory and Ronca [5,15] wedded the steric and Maier-Saupe approaches by incorporating anisotropic dispersion forces into the hard-rod calculations of the Flory lattice model [4]. Further progress with the task has been made by Warner, who calculated the mean field that a rod ''sees'' in a fluid of other rods with which it interacts via both anisotropic dispersion and steric repulsive forces [6,16,17]. There is no longer any doubt that both the anisotropic attractive *and* repulsive interactions are necessary to describe the isotropic-nematic transition in thermotropic liquid crystals.

There are three fundamental theories of translational diffusion in the nematic phase [10,18,19]. Franklin based his theory on hydrodynamics of the nematic phase and expressed the principal components of the diffusion tensor, $D_{\parallel}$ and $D_{\perp}$, the diffusion components parallel and perpendicular to the nematic director, in terms of the nematic order parameter S, molecular shape anisotropy, and viscosity coefficients [18]. Chu and Moroi calculated the components of the self-diffusion coefficients from a parametrized form of the momentum autocorrelation function in the limit of perfectly ordered clusters [19]. Diogo and Martins's approach to diffusion in the nematic phase is based on the concept of the free volume [10].

However, although the nematic potential used in the theories of molecular dynamics accounts, to some extent, for effects associated with the shape anisotropy of nematogen molecules (cf. Ref. [15]), the presence of steric interactions in the molecular dynamics of thermotropic nematogens has not received appropriate attention. Our basic idea, therefore, is to consider translational diffusion combining the free-volume mechanism of diffusion with the Flory lattice model of the nematic phase.

II. THEORY

Combined use of both models is particularly suitable for studying diffusion of a small solute (probe) molecule in the nematic phase. To evaluate the translational diffusion coefficients of the solute we assume that it is present in the nematic system in trace amounts only, i.e., its introduction does not alter the thermodynamic properties of the neat nematic system. We assume also that the probe molecule is spherical, its diameter being the same as the width of the rodlike nematogen molecule. In the proposed theory we follow the generalized free-volume concept of Turnbull and Cohen and assume that the tracer is confined to a cage formed by the nearest mesogenic neighbors [8–10,12]. The tracer rattles inside the cage until fluctuations in density (redistribution of the free volume within the liquid) create a large enough void to permit a substantial translation of the tracer. There is di-

*Electronic address: UFMOSCIC@cyf-kr.edu.pl

rect evidence of the existence of such voids with dimensions several times larger than the molecular size from computer simulations [20] and in the simple mechanical analogs of three-dimensional hard-sphere assemblies [21]. The large-scale diffusion coefficient can be written as [8]

$$D=\int_0^\infty D(v)p(v)dv, \tag{1}$$

where $v=w-w_0$, w, and w_0 are the cage free volume, the cage overall volume, and the probe van der Waals volume, respectively; $p(v)$ is the probability density of occurrence of v. $D(v)$ (the small-scale diffusion coefficient) is an apparent contribution to the overall diffusion arising from the diffusion in a cage.

Although density fluctuations produce cages of an arbitrary shape, the minimum model requirement is to enable probe displacement by l, i.e., to provide an instantaneous unobstructed tubelike path (free path), with the tube diameter the same as that of the tracer, d_t and $l+d_t$ in length. The remaining part of the cage, excluding the tubelike path, is unimportant for the diffusion process and can be considered as part of the surrounding path medium. It is therefore a plausible assumption for the problem of diffusion that the redistribution of free volume creates randomly tubelike cavities around the tracer, the length and orientation of a given cavity being, in general, dependent on the tracers position.

It is inherent to the nature of the isotropic and nematic phases that the probability that the free path is formed in an arbitrary direction is uniform over space. Hence Eq. (1) can be rewritten as

$$D(\Omega)d\Omega=\int_{l^*}^\infty D(\Omega;l)p^0(l)dl\ d\Omega, \tag{2}$$

where $D(\Omega;l)d\Omega=D^0(l)g_l(\Omega)d\Omega$ is an apparent contribution arising from small-scale diffusion along the free path of length l and occupying the solid angle Ω with respect to a fixed reference direction in space. $p^0(l)$ is the probability density of finding the free path of length l and the geometric factor $g_l(\Omega)$ gives the probability of occurrence of this free path at the probe position along the direction Ω. We introduce as well a threshold free path l^* just large enough to permit the minimum countable displacement of the probe [8].

Cohen and Turnbull commented that the in-cage diffusion constant is only slowly varying with the cage size [8] and in what follows will be considered merely as a scalling factor [22] $D^0(l)=D^0(l^*)$. In the isotropic phase $g_l(\Omega)$ is uniform over 4π of the solid angle $g_l(\Omega)=(4\pi)^{-1}$. Individual random steps average out, resulting in macroscopic translation characterized by the diffusion coefficient [cf. Eq. (1)]

$$D_{\rm iso}=D^0(l^*)\int_{l^*}^\infty p^0(l)dl. \tag{3}$$

However, in the nematic phase the mesogen long axes are orientationally ordered and the formation of a cavity tube along the nematic director should be more frequent than of the one created perpendicular to it. In what follows, length is for convenience expressed in units of d_t, i.e., in axial ratio units. The probability that a free path of length l has direction Ω is equal to the conditional probability of finding a tubelike cavity of length $l+1$ surrounding the probe oriented in the Ω direction $P(l+1,\Omega)$ weighted by the probability that there is already an equilibrium cavity around the tracer [23], viz.,

$$g_l(\Omega)=g_l(\psi)=P(l+1,\psi)/P_t, \tag{4}$$

where P_t is the probability of finding the equilibrium cavity at the probe position. Due to the axial symmetry of the nematic phase, $g_l(\Omega)$ depends only on the angle between the free path axis and the director, ψ. Assuming that diffusion along the free path is still given by $D^0(l)=D^0(l^*)$, Eq. (2), using Eq. (4), yields the macroscopic diffusion coefficient in the direction ψ:

$$D_{\rm nem}(\psi)\sin\psi d\psi=D^0(l^*)\int_{l^*}^\infty g_l(\psi)p^0(l)dl\sin\psi d\psi. \tag{5}$$

Equation (5) can now be used to obtain the two principal components of the nematic phase diffusion tensor, $D_\parallel$ and $D_\perp$, i.e., parallel ($\parallel$) and perpendicular ($\perp$) to the director, respectively. Projecting small-scale diffusion onto both directions and averaging over all possible orientations we have [24]

$$D_\parallel=\langle D_{\rm nem}(\psi)\cos^2\psi\rangle_\psi, \tag{6}$$

$$D_\perp=\tfrac{1}{2}\langle D_{\rm nem}(\psi)\sin^2\psi\rangle_\psi, \tag{7}$$

where the subscript ψ emphasizes averaging over $0\leqslant\theta\leqslant\pi/2$ and the factor of 1/2 accounts for the uniaxial symmetry of the nematic phase.

To proceed further the probability functions $P(l,\psi)$ and P_t must be known [cf. Eq. (4)]. Benefiting from our past experience, we found that the Flory lattice method is particularly suitable for evaluating these probabilities [25]. In the usual way, the volume occupied by the nematic phase of monodisperse rodlike molecules is subdivided into a cubic array of linear dimension equal to the diameter of the ''solvent'' particle and the width of the ''solute'' rod. All sites of the lattice are occupied in such a way that each rod is constrained to consist of contiguous fully occupied x cells, x being the rod length-to-diameter axial ratio. The solvent particles fully occupy the remaining cells.

For our purpose, the free volume within the neat nematic liquid, i.e., the difference between the liquid volume and the volume of its van der Waals limit, will be treated as a neutral ''solvent'' in the lattice, the amount of which can be adjusted appropriately. Next, we introduce a few tracer molecules into the system, whose size is that of the lattice unit cell, in such way that they can reside only in cells occupied by the free volume. We assume further that the tracers are neutral, i.e., they interact with the neighoring particles via steric repulsions only and are thus a thermodynamically indistinguishable part of the solvent.

As mentioned already, we expect that the way in which the free volume is distributed over the sample volume reflects the order of the nematic liquid. We assume that free-volume cavities are tubelike empty shells whose diameter is equal to the lattice unit cell and are polydisperse in the

length. Their polydispersity will be represented by the ratio of the number n_l of cavities with axial ratio l to the total number n_c of the cavity ''particles'' in the system, which has already been introduced as the probability of occurrence of the free path of length l, $p^0(l)=n_l/n_c$ [cf. Eqs. (2) and (5)].

All mesogens are assumed to interact with each other via steric repulsions on contact as well as via Maier-Saupe dispersion forces. The tubelike cavities, on the other hand, interact with each other and with mesogens only sterically.

The latter assumption, although it seems artificial, is, however, equivalent to the more physically plausible assumptions that (i) the volume of the sample remains constant (thus the free volume is also constant), i.e., the free-volume tubes cannot overlap and the only process allowed is redistribution of the free volume within the sample, so (ii) the free-volume tubes are built up from empty sites on the Flory lattice in the same way the mesogen molecules are built from occupied sites. The argument proceeds as follows.

The reference state in the Flory method is the state of perfect orientational order ($S=1$) of rodlike particles along one of the lattice axes, say **Z**. A solution of monodisperse rods in the nematic state ($S<1$) is then represented by a perfectly ordered solution of polydisperse in length *subparticles* resulting from replacing each solute molecule by several subparticles, their number and length depending on the rod inclination from **Z**. In any row parallel to **Z** the distribution of subparticles and vacant sites (free volume) is random and is uninfluenced by conditions in neighboring rows [4]. It is therefore a plausible expectation that when scanning along each row we encounter indigenous sequences of empty sites of random length. Our assumption that the free-volume tubes interact sterically with each other and with mesogens introduces a constraint to this randomness that the vacant sites in each row are clustered to form a polydisperse in length *subtubes* in accord with the free-volume tube orientation and length distribution function. This modification is in close agreement with the founding ideas of the free-volume theory [9], and of the nematic state theory of Cotter [26]. We believe, therefore, that the artificiality of the assumption is no worse than those intristic to the lattice and free-volume theories.

For each species of the same length, the orientational distribution function results from the orientational equilibrium they attain with other rods of the system. Application of the Flory lattice formalism yields the equilibrium orientational distribution functions

$$f_l(\psi)=f_l'\exp[-A_{\overline{y},x_{\rm eff}}(l-1)\sin\psi] \tag{8}$$

for l species of the cavity shells and

$$f_x(\psi)=f_x'\exp[-A_{\overline{y},x_{\rm eff}}(x-1)\sin\psi]\exp\left(\frac{3}{2}c_xS_x\frac{xT^*}{T}\sin^2\psi\right), \tag{9}$$

for the monodisperse mesogen rods x. S_x and $\overline{y}$ are equilibrium values of the nematic order parameter and the Flory disorder index, respectively, i.e., the mean projection of the system rod onto the plane normal to the director; $A_{\overline{y},x_{\rm eff}}=-4\ln(\overline{y}/x_{\rm eff})/\pi$, $x_{\rm eff}$ being the rod average axial ratio in the system (i.e., averaged over rodlike molecules and cavities); xT^* defines the scale of the mesogen-mesogen interaction (in units of absolute temperature) and is usually found by fitting the theory to the clearing point, T_{NI} of the particular system [17]. f_l' and f_x' are inherent to the theory scaling parameters [5,15]. T is the system (absolute) temperature and c_x denotes the volume fraction of the mesogen rods. It should be noted that Eq. (8) and the first exponent in Eq. (9) arise purely from steric effects. The second exponent in Eq. (9), which is absent in Eq. (8), results from the dispersion forces present between the nematogen rods.

Equation (8) gives the required probability $P(l,\psi)=f_l(\psi)$ that the cavity of length l is declined by ψ from the director. We find the remaining unknown probability P_t by assuming that the equilibrium cage surrounding the probe is equal to the lattice unit cell. It is easily obtained by setting l to 1 in Eq. (8):

$$P_t=f_1(\psi)=f_1'. \tag{10}$$

With the aid of Eqs. (8) and (10) one can now evaluate the conditional probability that the free path of length l (axial ratio units) is created at the position of the probe in the direction ψ, $g_l(\psi)$ [cf. Eq. (3)]:

$$g_l(\psi)=P(l+1,\psi)/P_t=\text{const}\times\exp(-A_{[\overline{y};x_{\rm eff}]}l\sin\psi). \tag{11}$$

One of the important concepts of the free-volume theory is to make the free volume temperature dependent [8]. The free volume in the sample is assumed to arise from the thermal expansion at constant pressure, which gives, for the average free volume per rod l_f,

$$l_f=\alpha(T-T_g)x \tag{12}$$

or, in terms of the volume fraction of the system occupied by the free volume,

$$c_f=1-c_x=\frac{\alpha(T-T_g)}{1+\alpha(T-T_g)}, \tag{13}$$

where α is the linear thermal expansion coefficient and T_g is the glass temperature, i.e., the temperature at which system reaches its van der Waals limit. In the absence of clear experimental evidence to the contrary, we assume that T_g is characteristic for the bulk material rather than for the diffusion process, i.e., we assume that it does not depend on the direction of diffusion (cf. below).

The temperature-dependent free volume influences the diffusion coefficient in the nematic phase in two distinct ways. First, it makes the free path distribution function $p^0(l)$ temperature dependent [cf. Eq. (2)]. Simple considerations lead to [8,10–12]

$$p^0(l)=[l^*\alpha(T-T_g)]^{-1}\exp\{-l/[l^*\alpha(T-T_g)]\}, \tag{14}$$

where l^* is the threshold free path [cf. Eq. (2)]. Second, as $p^0(l)$ and c_f vary with temperature the orientational equilibrium of the rod-cavity mixture changes by changing the relative concentration of rods and cavities in the system, as measured by the equilibrium constants S_x, $\overline{y}$, and $x_{\rm eff}$. The latter two enter into the factor $A_{\overline{y},x_{\rm eff}}$ in Eq. (8); therefore, although

the steric exponent in Eq. (8) is explicitly temperature independent, a subtle dependence on temperature enters into the $f_l(\psi)$ $[\equiv P(l,\psi)]$ exponent through the equilibrium values of $A_{\overline{y},x_{\rm eff}}$.

Substitution of $p^0(l)$ [Eq. (14)] and $g_l(\psi)$ [Eq. (11)] into Eq. (5) yields, upon integration,

$$D_{\rm nem}(\psi)\sin\psi d\psi = \hat{D}_0[\alpha\gamma l^*(T-T_g)]^{-1} \times \exp(-\gamma l^*)\sin(\psi)d\psi, \qquad (15)$$

where $\gamma=(4/\pi)\ln(\overline{y}/x_{\rm eff})\sin\psi+[\alpha l^*(T-T_g)]^{-1}$ and the constant $\hat{D}_0$ incorporates the scaling factors of the theory [cf. [22] and Eq. (11)]. In general, there are no quantitative data on the diffusion anisotropy in liquid crystals of high quality and the anisotropy is customarily represented by a dimensionless diffusion ratio $D_\parallel/D_\perp$. Therefore, $\hat{D}_0$ cannot be compared directly with experiment and we omit its detailed evaluation, considering it merely as a scaling factor.

III. CALCULATIONS

In order to examine the effect of various parameters on the translational diffusion anisotropy we specialize the above result to values of the axial ratio and thermal expansion coefficient typical of nematogens. Detailed caculations require specification of the values of the parameters appearing in the theory. They are either defined from experimental data (x,α,T_g) or obtained by fitting the theory to experimental data (T^*). If particular values of l^* and T are then chosen, values of $\overline{y}$ and $x_{\rm eff}$ result from the self-consistency condition of the Flory theory.

Calculations proceeded as follows. For a given set of experimentally determined values $\{x,\alpha,T_{NI},T_g\}$ a trial value of l^* is selected, thus $p^0(l)$, c_f, and $x_{\rm eff}$ become quantitatively defined [cf. Eqs. (14) and (13)]. Next, the equilibrium parameters of the system in the nematic state at the nematic-isotropic transition are established numerically via the Flory method in the usual manner [25,17]. The theoretical transition temperature T^t_{NI} is then identified with the experimental clearing point T_{NI} and thus the last unknown parameter T^* is found, [cf., e.g., Eq. (7) of Ref. [17]]. This procedure fixes the temperature scale. The reduced temperature of interest T/T_{NI} below the clearing point is then selected. Since the temperature variation changes c_f and $x_{\rm eff}$ (i.e., via the rod axial ratio polydispersivity function), the new iteration parameter $T^{*\prime}$ is found by finding T^t_{NI} again for this new composition of the system. Only then do the self-consistent Flory method calculations yield the equilibrium value of $\overline{y}$ at T/T_{NI} and thus of $D_{\rm nem}$, whence $D_\parallel/\hat{D}_0$ and $D_\perp/\hat{D}_0$, or $D_\parallel/D_\perp$ may be calculated.

Several studies of the translational diffusion anisotropy dependence on different parameters were performed. First, the influence of the glass temperature on translational diffusion in the model nematogen was studied. For this purpose a *p*-methoxybenzlidene-*p′*-*n*-butylaniline (MBBA) like matrix is chosen. Although MBBA does not show in the nematic phase effects characteristic of the glass transition proximity, for this study we introduced such a hypothetical transition at $T_g=100$ K (220 K below $T^{\rm MBBA}_{NI}$). As expected,

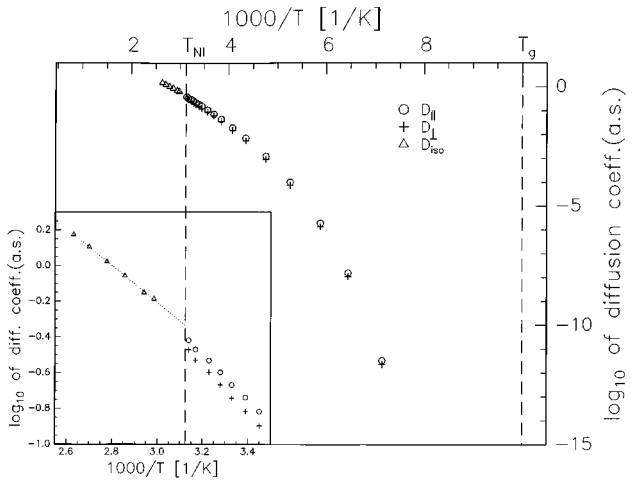

FIG. 1. Small tracer diffusion in the MBBA-like rodlike matrix with a hypothetical glassy transition: Arrhenius plot of $D_\parallel/\hat{D}_0$, $D_\perp/\hat{D}_0$, and $D_{\rm iso}/\hat{D}_0$ (a.s. denotes arbitrary scale). The inset shows diffusion constants over the usual temperature range of the nematic phase.

both principal diffusion coefficients clearly show a critical slowing-down of the diffusion process on approaching T_g (cf. Fig. 1). However, the anisotropy ratio seems nearly uninfluenced by T_g. Detailed calculations not presented here show that for T_g/T_{NI} increasing from 0 to 0.96, $D_\parallel/D_\perp$ increases, but the change does not exceed a few percent. This result is not surprising since the most pronounced dependence of the anisotropy ratio on temperature enters in our model through the orientational order dependence on temperature. The latter is weakly temperature dependent far away from T_{NI} and essentially uninfluenced by the glass temperature [27]. Therefore, in what follows, the dependence on T_g in Eqs. (13)–(15) is neglected.

In Fig. 2 the isothermal diffusion anisotropy ratio $D_\parallel/D_\perp$ in a MBBA-like matrix is shown as a function of the

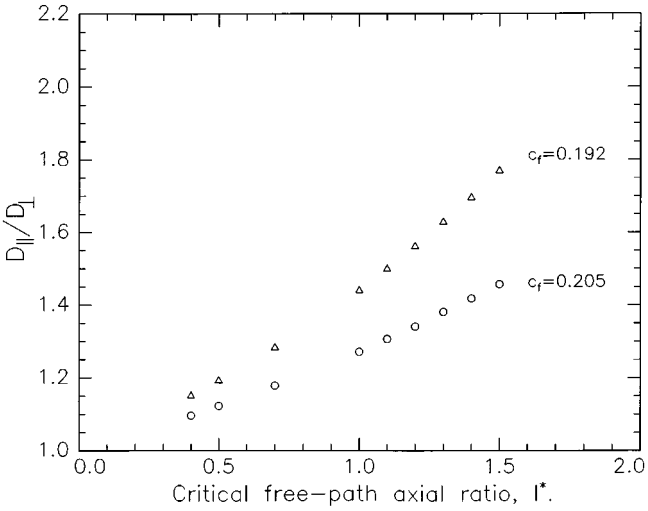

FIG. 2. Small tracer diffusion in the MBBA-like rodlike matrix: $D_\parallel/D_\perp$ as a function of the critical free path for two different temperatures $T/T_{NI}=0.995$ (○) and $T/T_{NI}=0.919$, (△). c_f is the free-volume fraction in the sample.

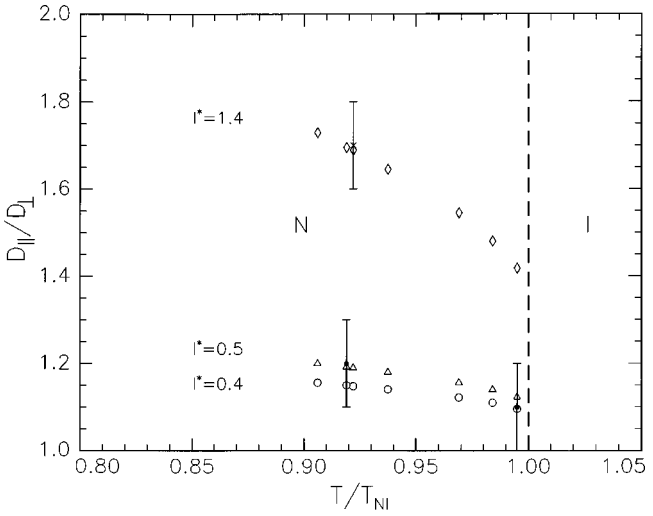

FIG. 3. Small tracer diffusion in the MBBA-like rodlike matrix: $D_\parallel/D_\perp$ as a function of reduced temperature for three different values of l^*. For comparison, experimental results are also shown for methane [26] (○) and MR diffusing in MBBA [27] (+).

critical free-path length l^* at two distinctively different temperatures in the nematic phase: $T/T_{NI}=0.995$, which is equivalent to the free-volume fraction of $c_f=0.205$, and $T/T_{NI}=0.919$, corresponding to $c_f=0.192$ [cf. Eq. (13)].

The results of calculations of $D_\parallel/D_\perp$ as a function of reduced temperature T/T_{NI} for a few values of l^* are shown in Fig. 3. Ranges of T/T_{NI} and l^* values (0.919–0.995) and (0.4., 0.5, and 1.4), respectively, are fitted to the experimental temperature range and experimental data on $D_\parallel/D_\perp$ of MBBA [28,29].

Finally, in Fig. 4 the diffusion anisotropy is shown as a function of the host molecule axial ratio. For this purpose we selected seven typical thermotropic nematogens, the axial ratio of which ranged from $x=3.6$ to 5.2 [15]. Unfortunately,

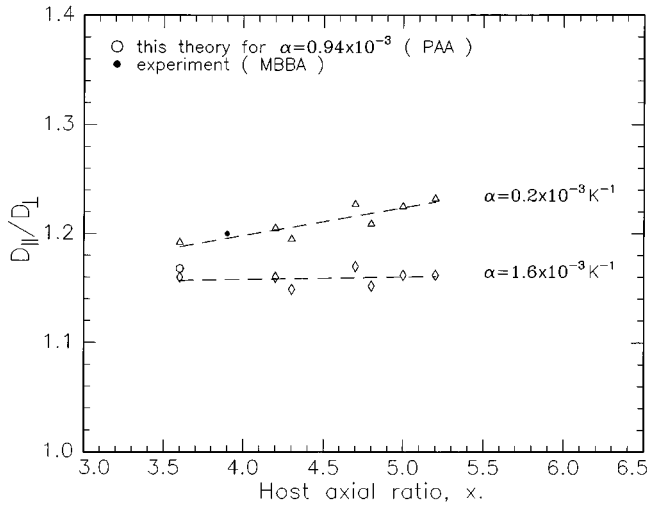

FIG. 4. Small tracer diffusion in different rodlike matrices, at $T_{NI}-26$ K, $l^*=0.4$, and two limiting values of α: 16×10^{-4} K^{-1} (◇) and 2×10^{-4} K^{-1} (△). ○ is the numerical result for PAA parameters (i.e., $\alpha=9.4\times10^{-4}$ K^{-1} [29]), and ● is the experimental result for MBBA [27].

the volume thermal expansion coefficient is known only for PAA in this set of nematogens, $\alpha=9.4\times10^{-4}$ [30]. In order to get a reasonable estimate of a general trend in the $D_\parallel/D_\perp$ dependence on x, we considered two limiting experimental values of α; 0.2×10^{-3} and 1.6×10^{-3} K^{-1} [30].

IV. DISCUSSION

The results shown in Figs. 2–4 all are representative for the most typical values of the axial ratio $x=3.6-5.2$ [15] and thermal expansion coefficient $\alpha=(2-16)\times10^{-4}$ K^{-1} [30] for nematogens. The temperature-dependent study is specialized to MBBA, a ''classic'' room-temperature nematogen for which parameters are reasonably well established, $x^{\mathrm{MBBA}}\simeq3.9$, $\alpha^{\mathrm{MBBA}}\simeq8\times10^{-4}$ K^{-1} [31], and $T_{NI}^{\mathrm{MBBA}}=320$ K [30], and for which diffusion data are available for different tracers [28,29]. Unfortunately, diffusion data in nematogens obtained by different methods are very inconsistent with each other [cf. Figs. 9 and 10 of Ref. [32]], and a comparison between theory and experiment can at best be made only semiquantitatively.

The most interesting problem we tried to address is the critical (or threshold) free-path length, sufficient for the minimum countable displacement of the probe, which is the fundamental parameter in the free-volume approach to diffusion [10,11]. Inspection of Fig. 2 reveals that the anisotropy ratio $D_\parallel/D_\perp$ is indeed quite sensitive to the critical free-path length l^*, increasing rather dramatically as l^* increases. Furthermore, the increase is more pronounced at lower temperatures. A comparison of this result with experimental data on $D_\parallel/D_\perp$, which ranges from 1 to about 4 depending on the tracer size, its size compatibility with the solvent molecule size, and also tracer concentration [31] shows that the critical free path for a small spherical probe should not exceed 1–1.5, i.e., it should be of the order of the probe size. This is very well demonstrated in Fig. 3, where we compare the calculated anisotropy ratio vs normalized temperature with the available experimental data for tracer diffusion in MBBA [28,29]. On the one hand, we find that diffusion of a small methane molecule in MBBA [28] is well modeled by our theory with $l^*\simeq0.4-0.5$. On the other hand, description of diffusion of a larger methyl red (MR) molecule requires $l^*\simeq1.4$ or so. Both tracers are nearly spherical, but while the diameter of methane is half of the host molecule width, the diameter of MR is comparable with the width. Thus, by comparing l^* with the diffusant size we get the intuitively acceptable result that the minimum countable step corresponds to the diffusant size [8].

The temperature dependence of $D_\parallel/D_\perp$ shown in Fig. 3 reflects first of all the increasing orders of the system on lowering the temperature. The predicted rate at which $D_\parallel/D_\perp$ changes with temperature decreases as the temperature falls away from T_{NI}, as a consequence of the temperature dependence of the free-path orientational distribution function. Not surprisingly this effect is less pronounced for small displacements (0.4,0.5) than for larger ones (1.4), since the probability of creation of short free-path tubes is more uniform over the whole solid angle than for the longer tubes. Although the calculated rate seems to be somewhat smaller than that observed experimentally, differences between theo-

retical and experimental curves remain within experimental error, e.g., for methane in MBBA [28] (cf. Fig. 3). Such a weak temperature dependence of the anisotropy ratio is characteristic for nearly all results of translational diffusion anisotropy studies [31]; it is routinely found for both tracer and self-diffusion that away from T_{NI} the temperature dependence of the principal diffusion coefficients in the nematic phase $D_{\parallel}$ and $D_{\perp}$ is Arrhenius-like, with the difference between the two activation energies lying within experimental error.

We found it interesting to compare diffusion of the same spherical tracer in different rodlike nematic solvents (cf. Fig. 4). In the absence of sufficient experimental data we considered model solvents with two limiting values of the thermal expansion coefficient. $D_{\parallel}/D_{\perp}$ increases essentially linearly with the solvent axial ratio x, the increase being somewhat more rapid for smaller α. Experimental data should then fall within these boundary lines, as shown in Fig. 4 for PAA (predicted) and MBBA (experimental). Nevertheless, the increase is weak, i.e., no more than 10% for x increasing from 3.5 to 5.5. This is in good quantitative agreement with experimental results, showing very similar values of the anisotropy ratio in different nematic solvents.

Although the theory does not address the isotropic phase, we find it interesting to compare the diffusion coefficient behavior in the nematic and isotropic phases. First of all, the self-consistency test showed that in the absence of the nematic ordering the diffusion anisotropy diminishes as expected. The calculated normalized diffusion coefficient in the isotropic phase $D_{\mathrm{iso}}/\hat{D}_0$ shows a typical Arrhenius behavior in temperature (cf. Fig. 1). On extrapolating to the isotropic-nematic phase transition we find, however, a non-negligible jump in the diffusion coefficient values in the isotropic and nematic phases. Although the difference is small, such a result is in a good agreement with experimental results as well as theoretical predictions of Tao *et al.* [33]. A quantitative comparison is beyond the scope of the present paper, but we want to emphasize that both theories account for the orientation-dependent component of the density (in our case, the free volume). In the present theory that contribution to the density enters the equilibrium orientational distribution function via the parameters x_{eff}, $\overline{y}$, and T^* with particular values depending on the form of the spatial distribution of the cavities. In summary, our model shows good quantitative agreement with the available experimental data for tracer diffusion in nematic solvents, for diffusants comparable in size to the width of the matrix molecules.

ACKNOWLEDGMENTS

This work was supported by the Polish State Committee for Scientific Research (KBN) Grant No. 2 P03B 210 08 and EC Human Capital and Mobility Network Contract No. ERBCIPDCT940607. We are indebted to Dr. Keith Earle for many helpful discussions.

[1] J.D. Weeks, D. Chandler, and H.C. Andersen, J. Chem. Phys. **54**, 5237 (1971).
[2] J.A. Baker and D. Henderson, Annu. Rev. Phys. Chem. **23**, 438 (1972).
[3] H.C. Andersen, D. Chandler, and J.D. Weeks, Adv. Chem. Phys. **34**, 105 (1976).
[4] P.J. Flory, Proc. R. Soc. London Ser. A **234**, 73 (1956).
[5] P.J. Flory and G. Ronca, Mol. Cryst. Liq. Cryst. **54**, 289 (1979).
[6] M. Warner, Mol. Cryst. Liq. Cryst. **80**, 79 (1982).
[7] M. Wnek and J.K. Moscicki, Phys. Rev. E **53**, 1666 (1996).
[8] M.H. Cohen and D. Turnbull, J. Chem. Phys. **31**, 1164 (1959).
[9] M.H. Cohen and G.S. Grest, Phys. Rev. B **20**, 1077 (1979).
[10] A.C. Diogo and A.F. Martins, J. Phys. (Paris) **43**, 779 (1982).
[11] Y.-K. Shin, J.K. Moscicki, and J.H. Freed, Biophys. J. **58**, 445 (1990).
[12] J.K. Moscicki, Y.-K. Shin, and J.H. Freed, J. Chem. Phys. **99**, 634 (1993).
[13] L. Onsager, Phys. Rev. **62**, 558 (1942).
[14] W. Maier and A. Saupe, Z. Naturforsch. Teil A **14**, 882 (1959).
[15] P.J. Flory and G. Ronca, Mol. Cryst. Liq. Cryst. **54**, 311 (1979).
[16] M. Warner, J. Chem. Phys. **73**, 5874 (1980).
[17] M. Warner, Mol. Cryst. Liq. Cryst. **80**, 67 (1982).
[18] W. Franklin, Phys. Rev. A **11**, 2156 (1975).
[19] K.-S. Chu and D.S. Moroi, J. Phys. (Paris) Colloq. **36**, C1-99 (1975).
[20] P.L. Fehder, C.A. Emeis, and R.P. Futrelle, J. Chem. Phys. **54**, 4921 (1971).
[21] D.J. Bernal, Proc. R. Soc. London Ser. A. **280**, 299 (1964).
[22] A detailed disussion of $D^0(l)$ is beyond the scope of this paper. We note only that for $l \geqslant l^*$ one may estimate $D^0(l) \simeq D^o(l^*)$ as proportional to $l^* v_t = l^{*2}/\triangle t$, where v_t and $\triangle t$ are the probe in-cage mean velocity modulus and the time of displacement, respectively, both resulting from the particular shape of the cavity and from the probe interactions with the neighborhood. While we are not able at present to propose an analytical expression for $D^0(l^*)$, we plan to address the problem in a wider context in a future work; cf. [12].
[23] J. Han and J. Herzfeld, Biophys. J. **65**, 1155 (1993).
[24] G. Vertogen and W.H. de Jeu, *Thermotropic Liquid Crystals, Fundamentals* (Springer, New York, 1988).
[25] J.K. Moscicki, Adv. Chem. Phys. **63**, 631 (1985).
[26] M.A. Cotter, in *The Molecular Physics of Liquid Crystals*, edited by G.H. Luckhurst and G.W. Gray (Academic Press, London, 1979), Chap. 7.
[27] V.K. Dolganov, R. Fouret, C. Gors, and M. More, Phys. Rev. E **49**, 5230 (1994).
[28] M.E. Moseley and A. Loewenstein, Mol. Cryst. Liq. Cryst. **90**, 117 (1982).
[29] F. Rondelez, Solid State Commun. **14**, 815 (1974).
[30] A.P. Kapustin, *Experimental Studies of Liquid Crystals* (Nauka, Moscow, 1978); F. Noack, Mol. Cryst. Liq. Cryst. **40**, 103 (1977).
[31] G.J. Krüger, Phys. Rep., **82**, 229 (1982).
[32] F. Noack, Mol. Cryst. Liq. Cryst. **113**, 247 (1984).
[33] R. Tao, P. Sheng and Z.F. Lin, Phys. Rev. Lett. **70**, 1271 (1993).